World Academy of Science, Engineering and Technology
International Journal of Civil and Environmental Engineering
Vol:11, No:7, 2017

Torsional Rigidities of Reinforced Concrete Beams Subjected to Elastic Lateral Torsional Buckling

Ilker Kalkan, Saruhan Kartal

***Abstract*—**Reinforced concrete (RC) beams rarely undergo lateral-torsional buckling (LTB), since these beams possess large lateral bending and torsional rigidities owing to their stocky cross-sections, unlike steel beams. However, the problem of LTB is becoming more and more pronounced in the last decades as the span lengths of concrete beams increase and the cross-sections become more slender with the use of pre-stressed concrete. The buckling moment of a beam mainly depends on its lateral bending rigidity and torsional rigidity. The nonhomogeneous and elastic-inelastic nature of RC complicates estimation of the buckling moments of concrete beams. Furthermore, the lateral bending and torsional rigidities of RC beams and the buckling moments are affected from different forms of concrete cracking, including flexural, torsional and restrained shrinkage cracking. The present study pertains to the effects of concrete cracking on the torsional rigidities of RC beams prone to elastic LTB. A series of tests on rather slender RC beams indicated that torsional cracking does not initiate until buckling in elastic LTB, while flexural cracking associated with lateral bending takes place even at the initial stages of loading. Hence, the present study clearly indicated that the un-cracked torsional rigidity needs to be used for estimating the buckling moments of RC beams liable to elastic LTB.

***Keywords*—**Lateral stability, post-cracking torsional rigidity, uncracked torsional rigidity, critical moment

I. Introduction

DIFFERENT modes of buckling (local, flexural, flexural-torsional, torsional, lateral-torsional and lateral-distortional buckling) are taken into consideration in the design of steel members, since most of the steel profiles are composed of thin components (flanges and webs). These thin-walled profiles possess lower flexural and torsional rigidities, and therefore, lower resistance to buckling compared to the stocky solid sections. Unlike thin-walled steel profiles, normal proportioned RC members (beams and columns) are much less liable to buckling modes of failure, since the stocky cross-sections of RC members possess much higher flexural and torsional rigidities. However, the increase in the strength of concrete and reinforcing steel and the application of new construction techniques (prestressed concrete) enables the engineers to use more and more slender members in RC structures. Lateral stability failures, i.e. LTB and lateral distortional buckling (LDB), which have been considered as secondary modes of failure in RC construction in the past, are becoming a cause of concern. A number of recent bridge collapse incidents in the US (Fig. 1) and different parts of the globe underscored the need for including the lateral stability as a primary mode of failure in concrete construction.

Ilker Kalkan and Saruhan Kartal are with the Department of Civil Engineering, Faculty of Engineering, Kirikkale University, 71450 Kirikkale, Turkey (e-mail: ilkerkalkan@kku.edu.tr, saruhankartal@kku.edu.tr).

(a) Power Road, Red Mountain Freeway in Mesa, Arizona [1]

(b) I-80 in Clearfield County, Pennsylvania [2]

Fig. 1 Recent concrete bridge girder stability failure incidents in US

The precast concrete beams are subjected to different loading and support conditions from their construction in the precast concrete production facilities until the completion of the superstructure. In production, handling, transportation and erection stages, a precast concrete beam has different loading and support conditions, and therefore, different resistance to buckling. For this reason, the instability failure of a precast concrete beam can be overcome by accurately estimating the buckling moments of the beam at different stages of construction.

The buckling moment of a beam, whose warping deformations are not restrained, is directly dependent on the product of the lateral flexural rigidity and the torsional rigidity of the beam. Consequently, accurate estimation of the LTB moment can only be achieved by accurate estimation of the lateral bending and torsional rigidities. The present study pertains to the torsional rigidities of rather slender RC beams, i.e. liable to elastic LTB, at the instant of buckling. Although the torsional behavior and rigidities of RC beams under pure torsional moments have been studied extensively, there are no studies in the literature known to the author on the torsional rigidities of RC beams at the instant of buckling. The present study aims at shedding light upon estimating the torsional rigidities of slender RC beams right before buckling, so that more accurate buckling moment estimates could be obtained. For this purpose, different torsional rigidity expressions, proposed by various researchers, were introduced in the following section. The analytical estimates from these equations were compared to the experimental values of RC beams at buckling, failed due to elastic LTB. Significant conclusions were reached and recommendations were made based on these conclusions.

II. Analytical Torsional Rigidity Expressions

The torsional rigidity of an RC beam depends on the presence of diagonal tension cracks in the beam. If the maximum torsional moment in a beam remains below the cracking torque (Tcr), the entire beam behaves as a solid and homogeneous body and the torsional moment is resisted by the shear stresses around the perimeter of the section. In this very stage, the contribution of the flexural and shear reinforcement to the torsional rigidity can be neglected and the uncracked torsional rigidity (GCu) reflects the resistance of the beam to the torsional moments. ACI 318M-05 [3] code presents the following equation for calculating the torsional moment of an RC beam, at which diagonal tension cracking initiates:

$$T_{cr} = 0.33 \cdot \sqrt{f_c^{'}} \cdot \left(\frac{A_{cp}^2}{p_{cp}} \right) \tag{1}$$

where f'c is the specified compressive strength of concrete in MPa; Acp is the area enclosed by the outside perimeter of the cross-section and pcp is the perimeter of this area. Equation (1) was developed by assuming that diagonal tension cracking initiates as soon as the principal diagonal tensile stress in the beam reached the tensile strength of concrete. The uncracked torsional rigidity can be obtained from the basic torsional rigidity expression (GCu) proposed by St Venant [4] for elastic and homogeneous bodies:

$$GC_u = \beta_c \cdot b^3 \cdot h \cdot G_c \tag{2}$$

where Gc is the modulus of rigidity of concrete; b and h are the width and height of the beam; and βc is St Venant's torsional constant. Based on the simplifications for the torsional constant βc [5]-[7], the following GCu expression can be used for estimating the torsional rigidity of a slender RC beam before the formation of diagonal tension cracks:

$$GC_u = \frac{b^3 \cdot h}{3} \cdot \left(1 - 0.63 \cdot \frac{b}{h} \right) \cdot G_c \tag{3}$$

The diagonal tension cracks render the concrete core of an RC beam ineffective, and therefore, the torsional rigidity is provided by an equivalent thin-walled tube along the perimeter of the cross-section in the post-cracking stage. This imaginary thin-walled tube is composed of the outer skin concrete, the longitudinal reinforcing bars and the closed stirrups. Using the space truss analogy of Rausch [8], several torsional rigidity expressions were developed by different researchers [9]-[12] for the post-cracking part of the torque-twist curve of an RC beam. Tavio and Teng [12] proposed the following torsional rigidity expression for RC beams:

$$GC_{cr} = \frac{4 \cdot \mu \cdot E_s \cdot A_o^2 \cdot A_{cp}}{p_o^2 \cdot \left(\frac{1}{\rho_l} + \frac{1}{\rho_s} \right)} \tag{4}$$

where Es is the modulus of elasticity of the reinforcing steel; Ao is the area bounded by the centerline of the shear flow zone; po is the perimeter of this area; ρl and ρs correspond to the volumetric ratio of the longitudinal and shear reinforcement, respectively, obtained from:

$$\rho_l = \frac{A_l}{A_{cp}} \tag{5}$$

$$\rho_s = \frac{A_t \cdot p_1}{A_{cp} \cdot s} \tag{6}$$

where Al is the area of the total longitudinal reinforcement in the cross-section; At is the cross-sectional area of one leg of a single stirrup; s is the stirrup spacing; and p1 is the perimeter of the area bounded by the centerline of a closed stirrup. The shear flow zone, first proposed by Hsu [11], corresponds to the equivalent thin-walled tube (the outer-skin concrete), which resists the torsional moments after the formation of diagonal tension cracks and the core concrete ceases to contribute to the torsional rigidity. Thickness of the shear flow zone (td) is calculated from:

$$t_d = \frac{4 \cdot T_a}{A_{cp} \cdot f_c^{'}} \tag{7}$$

where Ta is the applied torque. Equation (7) was obtained from the softened truss model.

The torsional rigidity value calculated from (4) is denoted as the torsional rigidity at cracking [12], which corresponds to the slope of the secant line connecting origin to the end of the cracking plateau on the torque-twist curve.

III. Analyzed Experimental Data

In the present analysis, the torque-twist data of the slender RC beams, tested by Kalkan [13], was used. The dimensions and material properties of the analyzed beams are shown in Table I. All of the beams tested by Kalkan [13] underwent elastic LTB. High-strength concrete was used in all beams to extend the elastic portion of the stress-strain curve of concrete. In this way, pure elastic concrete behavior was attained at the instant of buckling. The #3, #5, #8 and #9 reinforcing bars in the specimens correspond to the deformed steel bars with a nominal diameter of 9.525 mm, 15.875 mm, 25.400 mm and 28.575 mm, respectively. The yield strength of the #3 and #5 bars in the specimens was measured as 470 MPa and the yield strength value of the #8 and #9 bars as 440 MPa. Different from other specimens, flexural reinforcement with a measured yield strength of 360 MPa was used in specimen B18-2. Welded wire mesh was used in specimens to provide adequate shear strength throughout the course of loading.

IV. Comparison of the Analytical and Experimental Torsional Rigidities

The beams tested by Kalkan [13] were subjected to a single concentrated load at mid-span and the beam ends were simply supported in and out of plane. In other words, the lateral deflection and torsional rotation were restrained at the ends. Furthermore, the end supports were designed to allow warping deformations (Fig. 2), so that the buckling behavior was not affected from warping. The loading mechanism did not restrain lateral translation and torsional rotation of the load application point (Fig. 2).

Since the lateral deflection and torsional rotation increase from the end supports to mid-span under these loading and support conditions, the torsional moment is not uniform along the span. The support regions, where the torsional moment was maximum, underwent diagonal tension cracking due to torsion, at much earlier stages of loading than the mid-span region. As the lateral deflections and torsional rotations increased with the applied load, diagonal tension cracks formed in the vicinity of mid-span. Since different parts of the beam span underwent diagonal tension cracking at different stages of loading, the torsional rigidity of the beam experienced gradual (stepwise) reduction along the course of loading. In other words, the torque-twist curve of each specimen could be approximated to a series of linear segments due to this stepwise reduction. Fig. 3 illustrates the torque-twist curve of one of the specimens tested by Kalkan [13]. Fig. 3 includes the torque-twist data of the specimen B44-2 both before and after buckling.

TABLE I
ANALYZED BEAMS

Beam	Beam Dimensions Width (mm)	Height (mm)	Effec. depth (mm)	Length (mm)	Flexural Reinfor.	Concrete Material Properties Compressive Strength (MPa)	Modulus of Elasticity (GPa)
B18-2	40	460	388.6	3660	3#5	78.0	34.5
B22-1	40	555	475.0	3660	3#5&1#3	80.1	35.8
B30	65	760	647.7	6095	3#8	84.2	41.0
B36	65	915	789.9	6095	3#9	88.1	40.3
B44-1	75	1120	952.5	11890	4#8	58.4	30.7
B44-2	75	1120	952.5	11890	4#8	58.9	30.7
B36L-1	75	915	774.7	11890	4#8	54.5	29.6
B36L-2	75	915	774.7	11890	4#8	54.7	31.0

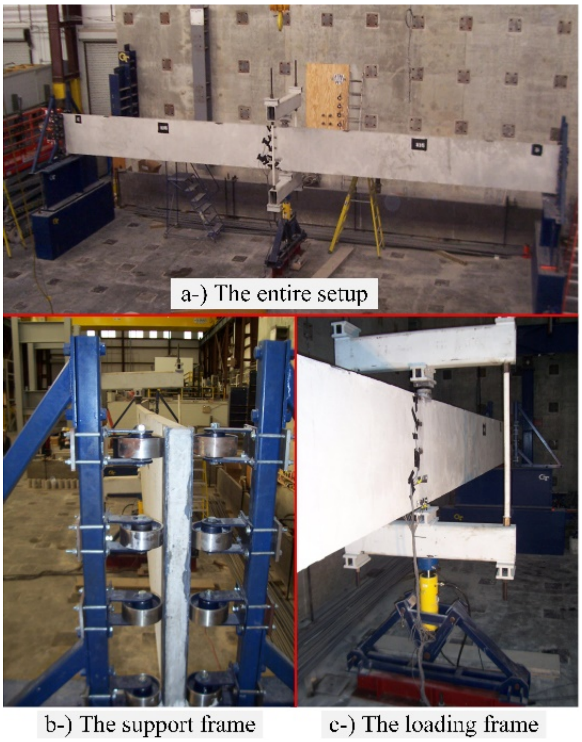

Fig. 2 Test setup used by Kalkan [13]

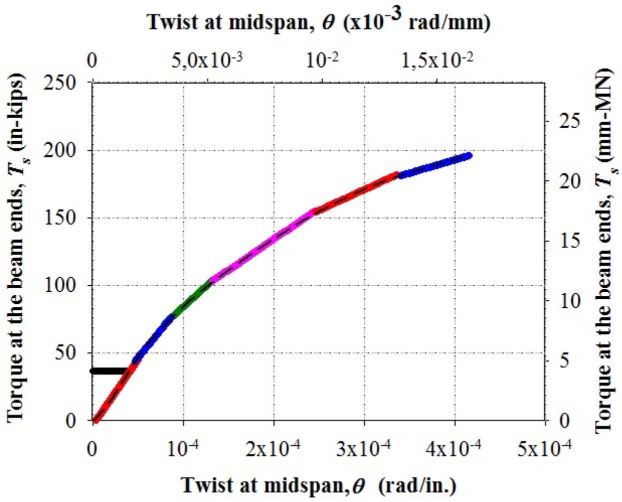

Fig. 3 Torque-twist data of specimen B44-2

The heavy solid line demarcates the pre- and post-buckling stages of the test. The torque-twist curves of the remaining specimens tested by Kalkan [13] were similar to the curve of specimen B44-2. As shown in Fig. 3, the heavy solid line (the maximum torsional moment in the beam at the instant of buckling) falls within the first linear segment of the torque-twist curve. This means that the beam were completely uncracked at the instant of buckling. In other words, there were no diagonal tension cracks in the entire span and the uncracked torsional rigidity was valid at the instant of buckling. The same conclusion can be drawn from Table II, which compares the experimental torsional rigidities (GC_{exp}) of the specimens with the uncracked (GC_u) and cracked (GC_{cr}) torsional rigidity values, calculated from (3) and (4), respectively. The experimental values of all specimens exceeded even the uncracked values, meaning that each and every specimen was completely uncracked at the instant of buckling. Consequently, the uncracked torsional rigidity represents the torsional rigidities of RC beams at the instant of buckling, failed by elastic LTB. The experimental values were greater than the uncracked torsional rigidity values due to the differential diagonal tension cracking in the span as a result of the non-uniform torsional moment distribution along the span.

TABLE II
EXPERIMENTAL AND ANALYTICAL TORSIONAL RIGIDITY VALUES

Beam	GC_{exp} (m^2.kN)	Calculated Values (m^2.kN)	
		GC_u	GC_{cr}
B18-2	26.2	5.9	1.0
B22-1	25.8	8.6	1.5
B30	88.8	59.5	8.1
B36	124.6	72.5	10.0
B44-1	154.8	108.9	16.7
B44-2	129.1	111.4	16.7
B36L-1	153.6	99.4	14.6
B36L-2	143.3	104.4	14.6

The maximum torsional moment in each beam at the instant of buckling (T_b) were compared to the cracking (threshold) torsion (T_{cr}) values, obtained from (1), in Table III.

TABLE III
MAXIMUM TORSIONAL MOMENT AND CRACKING TORQUE VALUES OF THE BEAMS

Beam	T_b (kN.m)	T_{cr} (kN.m)
B18-2	0.072	0.048
B22-1	0.054	0.062
B30	0.276	0.234
B36	0.157	0.290
B44-1	0.262	0.402
B44-2	0.206	0.403
B36L-1	0.306	0.343
B36L-2	0.284	0.343

As shown in Table III, the torsional moment in each and every beam at the instant of buckling remained below or slightly exceeded the cracking torque value, supporting the conclusion that the beams subject to elastic LTB remain completely uncracked in torsion up to buckling.

V. CONCLUSIONS

The torsional rigidities of slender RC beams at the instant of buckling were investigated in the present paper. The experimental torsional rigidity values of a set of eight slender RC beams tested by Kalkan [13] were compared to the analytical values from the uncracked and cracked torsional rigidity expressions for RC beams. Furthermore, the maximum torsional moments in the specimens at the instant of buckling were compared to the threshold (cracking) torsion values. The slender RC beams were found to be completely uncracked in torsion at the instant of buckling. Therefore, the uncracked torsional rigidity values need to be used in the buckling moment expressions to reach accurate buckling moment estimates in elastic LTB.

ACKNOWLEDGMENT

In the analyses of the present study, the torque-twist data of the beams tested by Dr. Ilker Kalkan during his doctoral studies under the supervision of Prof. Dr. Abdul-Hamid Zureick at Georgia Institute of Technology, School of Civil and Environmental Engineering were used. The financial support of Georgia Department of Transportation is gratefully acknowledged.

REFERENCES

[1] R. G. Oesterle, M. J. Sheehan, H. R. Lotfi, W. G. Corley, and J. J. Roller, *Investigation of Red Mountain Freeway bridge girder collapse*. CTL Group Project No. 262291 Final Report, Arizona Department of Transportation, Arizona, USA, 2007.

[2] A. H. Zureick, L. F. Kahn, K. M. Will, I. Kalkan, J. Hurff, and J. H. Lee, *Stability of precast prestressed concrete bridge girders considering sweep and thermal effects.* GDOT Project No. RP 05-15 Final Report, Georgia Department of Transportation, Atlanta, Georgia, USA, 2009.

[3] ACI Committee 318, *Building Code Requirements for Structural Concrete and Commentary (ACI 318M-05)*, American Concrete Institute, Farmington Hills, Michigan, U.S.A., 2005.

[4] B. de Saint-Venant, "Mémoire sur la torsion des prismes (lu à l'académie le 13 juin 1853) (in French)", Mémoires des Savants Etrangers, Mémoires Présentés par Divers Savants à l'Académie des Sciences, de l'Institut Impérial de France et Imprimé par son Ordre, v. 14, p. 233-560, 1856.

[5] C. Wang, *Applied elasticity*, McGraw-Hill Book Co. Inc., New York, pp. 85-89, 1953.

[6] S. P. Timoshenko and J. N. Goodier, *Theory of elasticity (International ed.)*, McGraw-Hill Book Co., New York, pp. 309-313, 1970.

[7] A. Siev, "The lateral buckling of slender reinforced concrete beams," *Magazine of Concrete Research (London)*, vol. 12, no. 36, pp. 155-164, 1960.

[8] E. Rausch, *Berechnung des eisenbetons gegen verdrehung* (*in German*), Ph.D. thesis, Technische Hochschule, Berlin, Germany,1929.

[9] P. Lampert, "Postcracking rigidity of reinforced concrete beams in torsion and bending," *ACI SP 35: Analysis of Structural Systems for Torsion*, pp. 385-433, 1973.

[10] T. T. C. Hsu, "Post-cracking torsional rigidity of reinforced concrete sections," *ACI Journal, Proceedings*, vol. 70, no. 5, pp. 352-360, 1973.

[11] T. T. C. Hsu, "Shear flow zone in torsion of reinforced concrete," *Journal of Structural Engineering, ASCE*, vol. 116, no. 11, pp. 3206-3226, 1990.

[12] Tavio and S. Teng, "Effective torsional rigidity of reinforced concrete members," *ACI Structural Journal*, vol. 101, no. 2, pp. 252-260, 2004.

[13] I. Kalkan, "Lateral torsional buckling of rectangular reinforced concrete beams," *ACI Structural Journal*, vol. 111, no. 1, pp.71-81, 2014.